Accepted Manuscript

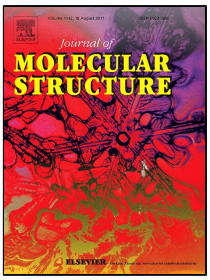

Design, synthesis, characterisation, conformation and biological investigation of *N*-acyl *r*-2,*c*-6-bis (4-methoxyphenyl)-*c*-3,*t*-3-dimethylpiperidin-4-ones

V. Mohanraja, S. Ponnuswamy

PII:	S0022-2860(17)30619-1
DOI:	10.1016/j.molstruc.2017.05.036
Reference:	MOLSTR 23777
To appear in:	*Journal of Molecular Structure*
Received Date:	07 March 2017
Revised Date:	05 May 2017
Accepted Date:	10 May 2017

Please cite this article as: V. Mohanraja, S. Ponnuswamy, Design, synthesis, characterisation, conformation and biological investigation of *N*-acyl *r*-2,*c*-6-bis (4-methoxyphenyl)-*c*-3,*t*-3-dimethylpiperidin-4-ones, *Journal of Molecular Structure* (2017), doi: 10.1016/j.molstruc.2017.05.036

Graphical Abstract

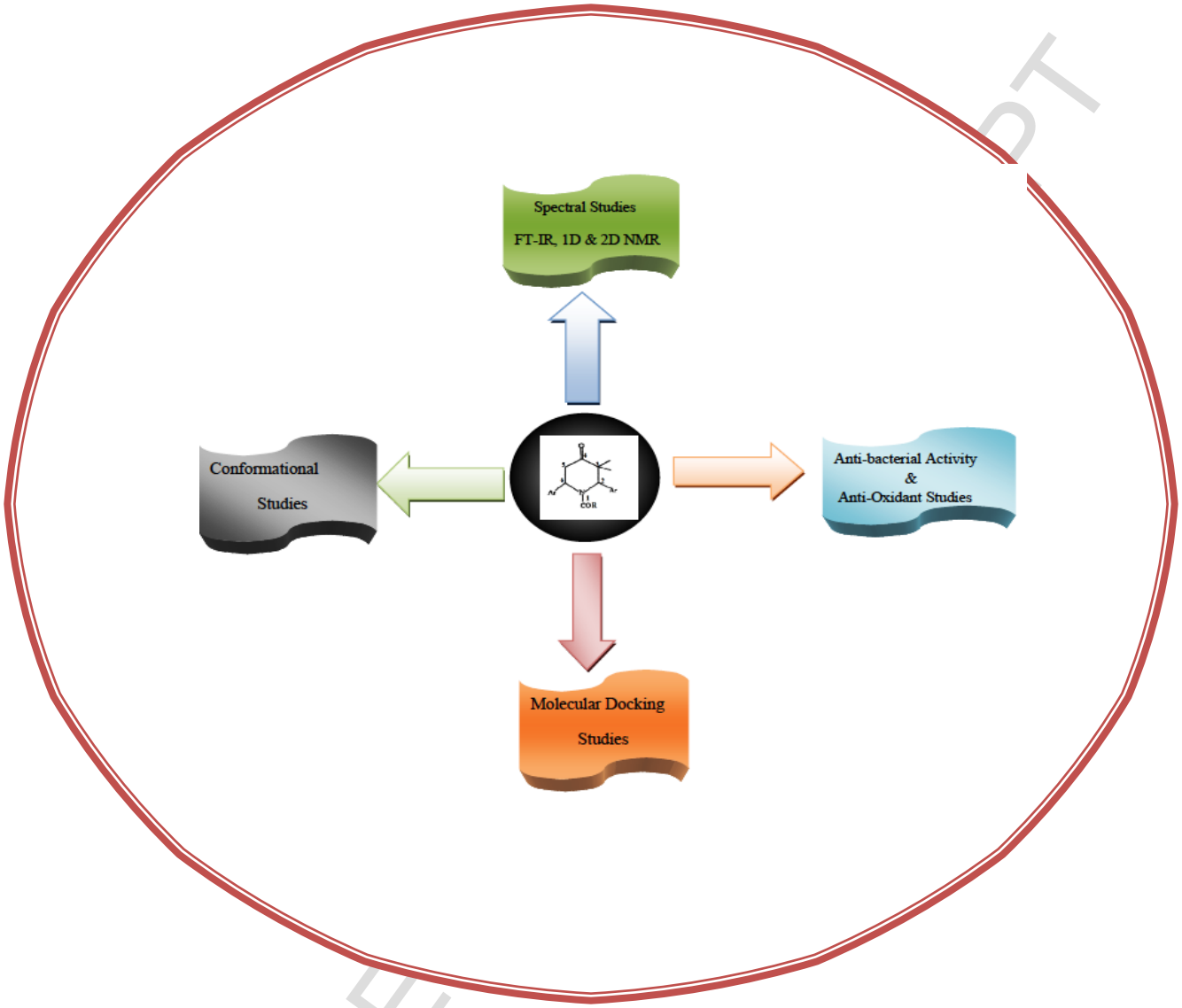

Highlights

- Five *N*-acyl piperidone-4-ones have been synthesized and characterized using NMR spectra.
- Compounds **2-5** prefer to exist in a distorted boat conformation **B1**
- Compounds **1-5** exhibit superior anti-bacterial activity against *pseudomonas species*
- Only moderate antioxidant activities have been observed for these compounds **1-5**
- Docking studies confirm the binding of these compounds with target protein CHK1.

Design, synthesis, characterisation, conformation and biological investigation of *N*-acyl *r*-2,*c*-6-bis (4-methoxyphenyl)-*c*-3,*t*-3-dimethylpiperidin-4-ones

V. Mohanraj[a,b] and S. Ponnuswamy [a]*

[a]P.G. & Research Department of Chemistry, Government Arts College (Autonomous), Coimbatore - 641 018, India.

[b] P.G. & Research Department of Chemistry, Sri Ramakrishna Mission Vidyalaya College of Arts and Science, (Autonomous) Coimbatore-641020, India.

Corresponding author : S.PONNUSWAMY,

Email: kspons2001@gmail.com

Mobile: +91- 9244645744

Abstract

In a wide research programme towards the study of piperidin-4-ones with efficient pharmacological effect, a new series of *N*-acyl *r*-2,*c*-6-bis(4-methoxyphenyl)-*c*-3,*t*-3-dimethylpiperidin-4-ones **2-5** are synthesised and characterized by IR spectra, ^{1}H, ^{13}C, DEPT - 135 and 2D (COSY and HSQC) NMR and mass spectra. The parent compound **1** prefers to exist in a chair conformation whereas the extracted coupling constant, chemical shifts and estimated dihedral angles show that the *N*-acyl piperdine-4-ones **2-5** prefer to exist in a distorted boat conformation $\mathbf{B_1}$ (with C_2 and C_5 in prow and stern positions) with coplanar orientation of *N*-C=O moiety. The existence of a fast *N*-CO rotational equilibrium between the boat conformations **B (I)** and **B (II)** has also been observed. Anti bacterial activity of the above test compounds **1-5** is determined against *pseudomonas sp.* and *salmonella sp.* The antioxidant activities are determined by the ABTS, DPPH and superoxide assays. Furthermore, molecular docking studies have been carried out for the compounds **1-5** with target protein CHK1.

Keywords: *N*-.Acylpiperidin-4-ones; NMR spectra; Distorted boat conformation; Antibacterial activity, Antioxidant activity, Molecular docking study.

1. Introduction

The development of new synthetic methods for use in organic synthesis is one of the areas of organic chemistry that has experienced a major renaissance during the recent past. There has been much interest in the synthesis of heterocyclic systems due to their varied physiological and biological activities **[1].** 2, 6-Disubstituted piperidines are the main constituents of a number of alkaloids which possess broad spectrum of biological activity **[2-10].** The 2,6-diarylpiperidin-4-ones and their derivatives have in recent years attracted considerable attention due to their possible bio-significance [**11-12].** The synthesis of compounds with attachment of electron withdrawing groups like NO, COR, etc., at nitrogen of a 2,6-disubstituted piperidine ring has been reported by our group, as well by others, to

bring major changes in the conformation of the ring and the orientation of the substituents **[8,10-15]**. The conformational preferences of piperidine ring are largely decided by the extent of resonance and magnitude of the resonance energy caused by the delocalization of nitrogen lone pair into the *N*-NO and *N*-C=O functions (**Fig.1**). The relative magnitudes of $A^{1,3}$-strain, torsional strain and 1,3-diaxial interaction are also the deciding factors **[16].** The *cis*-2, 6-diphenylpiperidin-4-ones with various substituents at 3 and 5 positions of the ring have been reported much earlier and they prefer to occupy a chair conformation with equatorial orientation of all the substituents **(Fig.2**). Though there appears in the literature more studies on the conformations of *N*-acyl-*cis*-2, 6-diphenylpiperidin-4-ones, to the best of our knowledge, no investigation has been performed on *N*-acyl-*r*-2, *c*-6-bis(4-methoxyphenyl)-*c*-3, *t*-3-dimethylpiperidin-4-ones**.**

In the present work, *r*-2,*c*-6-bis(4-methoxyphenyl)-*c*-3, *t*-3-dimethylpiperidin-4-one (**1**) and its *N*-phenylcarbamoyl, *N*-chloroacetyl, *N*-dichloroacetyl and *N*-morpholinoacetyl substituted compounds **2-5**, have been synthesized and their stereochemistry, studied using IR spectra, ^{1}H , ^{13}C and 2D (COSY and HSQC) NMR spectra and dihedral angle estimation by ratio method (DAERM) **[17].** DEPT spectra are also recorded for all the compounds to assist the assignment of ^{13}C NMR spectra. The mass spectra for the all compounds have been recorded to confirm the structure. The anti-bacterial activity studies on **1-5** have also been carried out. The X-ray crystal structure and the NMR spectral data show that the parent piperidin-4-one **1** prefers to adopt a chair conformation with equatorial orientation of anisyl groups **[13, 18]**. However, perusal of NMR data of the *N*-acyl compounds **2-5** reveals that all of them prefer to exist in a distorted boat conformation. All the compounds **1-5** are docked with **CHK1** protease protein using Schrodinger 9.5 software.

2. Experimental

2.1 Materials, methods and instruments

All the reported melting points were taken in open capillaries and are uncorrected. The IR spectra were recorded using a SHIMADZU FT-IR 884008 spectrometer using KBr pellets. The ^{1}H and ^{13}C NMR spectra were recorded in $CDCl_3$ solution at room temperature with a Bruker-AMX500 MHz NMR spectrometer, and the chemical shifts were referenced to TMS. A 0.05 M solution of the sample prepared in $CDCl_3$ was used for obtaining the 2D NMR spectra and the tubes used for recording the NMR spectra were of 5-mm diameter. Electron impact mass spectra were recorded using a JEOL GS mate spectrometer. Unless otherwise stated, all the reagents and solvents were of high grade and purchased from Sigma-Alrich chemicals, Bangalore, India and Merck chemicals, Worli, Mumbai. All the

solvents were distilled prior to use**.** The parent piperdin-4-one **1** was prepared by following the literature procedure **[19**].

2.2 Synthesis

2.2.1 Synthesis of *r*-2,*c*-6-bis(4-methoxyphenyl)-*c*-3,*t*-3-dimethylpiperidin-4-one (1)

3-Methylbutanone (10.7 ml, 100 mmol), *p*-methoxybenzaldehyde (24.2 ml, 200 mmol), and ammonium acetate (7.7 g, 100 mmol) were dissolved in 80 ml of distilled ethanol and heated over boiling water bath, with constant shaking until an yellow colour developed and changed into orange. The solution was left undisturbed for 14 hrs. The solid thrown out was filtered and purified by recrystallisation from ethanol.

2.2.2 *N*-Acyl piperidones 2-5: General procedure

The compounds **2-4** were prepared by the reaction of phenylisocyanate (1.6 ml, 15 mmol), chloroacetyl chloride (1.2 ml, 15 mmol) and dichloroacetyl chloride (1.5 ml, 15 mmol), respectively, on the *r*-2,*c*-6-bis(4-methoxyphenyl)-*c*-3,*t*-3-dimethylpiperidin.-4-one **(1**) (2 g, 5.9 mmol) in benzene medium using triethylamine (2 ml, 15 mmol) as a catalyst (**Scheme 1)**. The *N*-morpholinoacetyl piperidin-4-one **5** was prepared by the reaction of *N*-chloroacetylpiperidin-4-one **3** (2 g, 5 mmol) with morpholine (1 ml, 12 mmol) in benzene medium using triethylamine (2 ml, 15 mmol) as a catalyst. The reaction mixture for synthesis of **2-5** was stirred at room temperature for 6 h. The organic layer was separated, dried over anhydrous Na_2SO_4 and concentrated. The resulting product was purified by recrystallisation from benzene and pet-ether (60 - 80 ^oC) in a 2:1 ratio. Analytical data of the compounds **1-5** are reported in **Table 1.**

2.3 Anti-bacterial activity

2.3.1 Preparation of 24 hours old culture of test organism

Two human pathogenic bacterial strains *viz., pseudomononas species* and *salmonella species* have been used as test organism. 50 ml of Nutrient broth was prepared, sterilized and inoculated with the test organism. It was incubated at 37 ^oC for 24 hours. To determine antibacterial activity of test compounds, standard bacterial cultures of organisms 1.5 x 10^8cfu/ml were used. This was achieved by diluting the overnight test cultures with sterile nutrient broth until an O.D. value is obtained that is equivalent to the O.D. values of 0.5 Mcfarland standards. Further, this culture broth was diluted (i.e) 1:100 dilution to bring a count of 1.5 x 10^6 cfu/ml of the culture broth. Quantitatively the activities of the test

compounds **1-5** can be explained from the reduction in the OD values when compared to those of the DMSO control for each dilution [**20**].

2.4 Antioxidant activity of the compounds 1-5

2.4.1 DPPH$^{\bullet}$ method

The antioxidant activity of the compounds **1-5** is determined in terms of hydrogen donating or radical scavenging ability using the 1, 1-diphenyl-2-picrylhydrazyl stable radical DPPH, according to the method of Blois **[21]**. Various concentrations of samples were prepared and the volume was adjusted to 100 µl with methanol. 5 ml of 0.1 mM methanolic solution of DPPH was added and shaken vigorously. The tubes were allowed to stand for 20 minutes at 27 ºC. The absorbance of the sample was measured at 517 nm. Radical scavenging activity of the samples was expressed as IC_{50}. Concentration of the sample necessary to decrease initial concentration of DPPH$^{\bullet}$ by 50% (IC_{50}) under the experimental condition was determined. Lower value of IC_{50} indicates a higher antioxidant activity. Rutin and BHT were used as standard antioxidants in DPPH assay. The capacity to scavenge the DPPH radical was calculated using the following equation:

$$\text{DPPH Scavenging effect (\%)} = (\mathbf{A_0} - \mathbf{A_1}/\mathbf{A_0}) \times 100.$$

Where,

$\mathbf{A_0}$ =the absorbance of the standard;

$\mathbf{A_1}$ =the absorbance of the sample.

2.4.2 Antioxidant activity by ABTS$^{\bullet+}$ assay

The total antioxidant activity of the samples was measured by ABTS radical cation decolourisation assay according to the method of Re *et al.* **[22]**. ABTS$^{\bullet+}$ was produced by reacting 7 mM ABTS aqueous solution with 2.4 mM potassium persulfate in the dark for 12-16 h at room temperature. Prior to assay, this solution was diluted in ethanol (about 1:89, v/v) and equilibrated at 30 ºC to give an absorbance of 0.700±0.02 at 734 nm. The stock solution of the sample extracts were diluted such that after introduction of 10 µl aliquots into the assay, they produced between 20% and 80% inhibition of the blank absorbance. After the addition of 1 ml of diluted ABTS solution to 10 µl of sample or Trolox standards (final concentration 0-15 µM) in ethanol, absorbance was measured at 30 ºC exactly 30 minutes after the initial mixing. Appropriate solvent blanks were also run in each assay. Triplicate determinations were made at each dilution of the standard, and the percentage inhibition was calculated for the blank absorbance at 734 nm and then was plotted as a function of Trolox concentration. The unit of Trolox equivalent antioxidant

capacity (TEAC) is defined as the concentration of Trolox having equivalent antioxidant activity expressed as μM/g sample extract on dry matter.

2.4.3 Superoxide radical ($O_2^{\bullet-}$) scavenging activity

The assay was based on the capacity of the extracts to inhibit formazan formation by scavenging the $O_2^{\bullet-}$ generated in riboflavin-light-nitrobluetertrazolium (NBT) system [**23**]. Each 3 ml reaction mixture contained 50 mM sodium phosphate buffer (pH 7.6), 20 μg riboflavin, 12 mM EDTA, 0.1 mg NBT and 1 ml of sample solution (50-250 μg/ml). Reaction was initiated by illuminating the reaction mixture with different concentrations of sample extracts for 90 seconds. Immediately after illumination, the absorbance was measured at 590 nm. Identical tubes with reaction mixture kept in dark served as blanks. The percentage inhibition of superoxide anion generation was calculated using the following formula: % of inhibition = $[(A_0 - A_1)/A_0] \times 100$ where, A_0 is the absorbance of the control, and A_1 the absorbance of the extract/standard. The results were compared with the commercially available antioxidants such as rutin and BHT.

2.5 Molecular Docking Studies

Checkpoint kinase 1, commonly referred to as CHK1 is a serin/threonine-specific protein kinase, which in humans is encoded by the CHK1 gene CHK1 is required for the initiation of DNA damage checkpoints and has recently been shown to play a role in the normal cell cycle. In addition to mediating cell cycle checkpoints, CHK1 also contributes to DNA repair processes, gene transcription, embryo development, cellular responses to HIV infection and somatic cell viability. The DNA damage response is a network of signalling pathways that leads to activation of checkpoints, DNA repair and apoptosis to inhibit damaged cells from progressing through the cell cycle.

CHK1 protein was modeled computationally and its active sites were predicted using site map(Schrodinger 9.5) followed by docking studies. The preparation of the modeled CHK1 was achieved by a protein preparation wizard, piperidone and it was prepared using the ligprop program and docking procedure was performed using (XP) extra precision glide (Schrodinger 9.5) which produces the least number of inaccurate poses and calculate the accurate binding energy of the 3D structure of a known protein with a ligand. Docking studies were carried out using piperidone as an inhibitor against the model of CHK1 [**24**]**.**

3. Results and discussion

In the IR spectra of the compounds **2-5,** the amide >C=O stretching bands are observed at 1639 – 57 cm^{-1} in addition to the ring carbonyl stretching band at 1705-20 cm^{-1}. In the IR spectrum of the compound **2**, NH stretching band around 3265 cm^{-1} is absent and

the new NH (3301 cm^{-1}) and carbonyl stretching (1651 cm^{-1}) bands are observed due to the CONHPh moiety. The absence of N-H stretching band around 3265 cm^{-1} and the presence of additional carbonyl stretching band at approximately 1639-57 cm^{-1} in the IR spectra of the compounds **3-5** indicate the formation of **3-5**. In the mass spectra, the presence of molecular ion peaks at m/z 339, 458, 415, 449.85.and 424 for compounds **1-5**, respectively, and their fragmentation patterns confirm the structures of **1-5.** (**Table 1)**

The ^{1}H and ^{13}C NMR spectral data of *N*-acylpiperidin-4-ones **2-5** are presented in **Table 2**. Analysis of ^{1}H and ^{13}C NMR spectral data of the *N*-acylpiperidin-4-ones **2-5** shows the isochronous nature of proton and carbon signals at room temperature (**Figs. 3-4**). The ^{1}H NMR spectral signals of *N*-acylpiperidin-4-ones **2-5** are assigned based on their positions, multiplicities and intensities as well as in comparison with the parent amine **1**. In addition, COSY spectra are recorded for *N*-phenylcarbamoyl and *N*-chloroacetylpiperidin-4-ones, **2** & **3**, to confirm the assignments. Further, the unambiguous assignment of ^{13}C NMR signals for all the compounds **2-5** has been made using their DEPT spectra **(Fig. 5)**. The ^{1}H-^{13}C HETCOR spectra are also recorded **(Figs. 6-7)** to validate the assignment of ^{1}H and ^{13}C NMR signals. Analysis of ^{1}H & ^{13}C NMR spectral data of *N*-acylpiperidin-4-ones **2-5** indicates the preference for a non-chair conformation.

3.1 Orientation of N-C=O group

The *N*-C=O function may adopt either a coplanar or a perpendicular orientation with respect to the C_2-N-C_6 plane of the piperidine ring system. The *N*-acylpiperidin-4-ones **2-5** show the isochronous proton and carbon signals in their NMR spectra. If the delocalisation of the lone pair of electrons on the nitrogen of the *N*-acylpiperidin-4-ones **2-5** is sufficient to create a substantial double bond character along the *N*-CO bond, the adjacent carbons and protons may give rise to anisochronous signals as in the case of *N*-nitroso-*r*-2, *c*-6-diphenylpiperidines [**25**]. The absence of anisochronous signals in the RT NMR spectra of these *N*-acylpiperidin-4-ones **2-5** reveals that the *N*-CO group might adopt a coplanar orientation with the C_2-N-C_6 plane with very low *N*-CO rotational barrier ($\Delta G^{\#}$). The broadening of benzylic proton signals (H_2 & H_6) has been observed in the case of *N*-acylpiperidin-4-ones **3-5.** This broadening of α-proton signals may be due to the presence of rotational equilibrium about *N*-CO bond in these systems, which could be possible only in the coplanar orientation of the *N*-C=O moiety with respect to C_2-N-C_6 plane of the piperidine ring. Further, the absence of anisochronous signals in the *N*-acylpiperidin-4-ones **2-5** may be due to the low rotational barrier for the *N*-CO rotation compared to that of *N*-

NO. The α-proton signals in the case of *N*-phenylcarbamoyl piperidin-4-one **2** are not broad and it may be due to the lower rotational barrier for *N*-CONHPh moiety compared with other *N*-acyl functions [**26-27**] and to the extended conjugation through Ph-NH linkage of the phenylcarbamoyl group. The lower energy barrier of *N*-CONHPh function is due the increase in bulkiness of the substituent. Increase in the bulkiness of the substituents destabilises the planar ground state rather than the perpendicular transition state leading to a lowering of rotational barrier**.**

Further support for the coplanar orientation of N-C=O function in the compounds **2-5** can be derived from the ^{1}H and ^{13}C NMR spectral data of α-proton and carbon signals. The higher amount of deshielding of α-protons by 1 - 2.7 ppm and shielding of α-carbons by 4 - 7.5 ppm in *N*-acyl compounds **2-5** compared with the parent amine **1** support the coplanar orientation of N-C=O group. Hence, it may be concluded that the rotation about *N*-CO bond may be fast at room temperature compared to the NMR time scale and it results in a time averaged signal due to fast *N*-CO rotational equilibria. In addition, the reduction in the intensity as well as the number of Bohlmann bands **[28, 29]** around 2850 cm^{-1} in the IR spectra of the *N*-acylpiperidin-4-ones **2-5** compared to that of the parent amine **1** indicates that the lone-pair of electrons on nitrogen is in conjugation with *N*-C=O function which in turn could be possible only when the carbonyl groups in **2-5** are coplanar to the C_2-N-C_6 plane of the piperidine ring**.**

3.2 Conformation of the ring

The preferred conformation for the *N*-acyl compounds **2-5** has been arrived at by considering the vicinal coupling constants between the H_6 and H_{5a} & H_{5e} protons. The coupling constant values of the *N*-acylpiperidin-4-ones **2-5** have been extracted from their ^{1}H NMR spectra and are presented along with that of parent piperidin-4-one **1** in the **Table 3**. Except *N*-phenylcarbamoylpiperidin-4-one **2**, all the other *N*-acylpiperidin-4-ones show an unsymmetrical triplet for the H_6 benzylic proton instead of doublet of a doublet. However, for all these compounds **3-5**, the H_{5a} & H_{5e} protons show distinct double doublets. Hence the *cis* & *trans* vicinal coupling constants for the H_6 benzylic protons of *N*-acyl piperidin-4-ones **3-5** are extracted from its coupling partners H_{5a} & H_{5e}. In the case of *N*-phenylcarbamoylpiperidin-4-one **2**, the H_6 benzylic proton shows a doublet of a doublet. The H_2 benzylic protons in these compounds **2-5** show a singlet since these do not have a coupling partner at C3 **(Figs. 3 & 4).**

The vicinal coupling constant data of compounds **2-5** are employed to estimate the dihedral angles between the vicinal protons ($\phi_{cis} = \phi_{6a,5e}$ and $\phi_{trans} = \phi_{6a,5a}$) by DAERM and are presented in **Table 4**. Perusal of the data in the **Tables 2–4** led to the following observations: (i) there is a significant deshielding of benzylic protons at C_2 and C_6 positions. (ii) The H_2 benzylic protons are more deshielded than H_6 benzylic protons .There is a significant change in the vicinal coupling constants ($^3J_{6,\,5e}$ & $^3J_{6,\,5a}$) as well as dihedral angles when compared to the parent piperidin-4-one 1, indicating a preference for non-chair conformation. (iii) The C_2 and C_6 benzylic carbons are significantly shielded in the *N*-acyl compounds **2-5** compared with that of parent piperidin-4-one **1**. (iv) C_2 benzylic carbons are more shielded compared to C_6 benzylic carbons.

The preferred conformation of the *N*-acyl piperidin-4-ones **2-5** can be derived by using the above points. The parent piperidin-4-one **1** has been shown to prefer a chair conformation with equatorial orientation of aryl groups. The possible conformations for the *N*-acylpiperidin-4-ones **2-5** with coplanar orientation of N-C=O function are depicted in **Fig 8**. All these *N*-acylpiperidin-4-ones **2-5** show a similar trend in the spectral data when compared with its parent amine **1**. Hence the NMR spectral data of *N*-phenylcarbamoylpiperidin-4-one **2** is considered as a reference for discussion. In the chair conformation **CE** of *N*-phenylcarbamoylpiperidin-4-one **2,** which is similar to the parent amine **1**, the dihedral angles expected between H_6 benzylic proton and H_{5e} & H_{5a} protons are around 60° and 180°, respectively, ($\phi_{cis} = \phi_{6a,\,5e} \approx 60^o$ and $\phi_{trans} = \phi_{6a,5a} \approx 180^o$). However, the observed *cis* coupling constant ($^3J_{6a,5e}$) values of 6.0 Hz for the compound **2** (**Table 4**) and the corresponding dihedral angles of 44° (**Table 4**) could not be explained using the **CE** conformation. In addition, in the chair conformation **CE**, the benzylic protons at C_2 & C_6 occupy axial positions and are in the "out of plane" (shielding) region and the observed deshielding of $\Delta\delta$ = 2.72 & 1.05 ppm from that of the parent cannot be explained using the model proposed by Paulsen and Todt for the anisotopic effect of the amides [**30**]. Hence, the possibility of chair conformation **CE** is ruled out.

The >N–C=O moiety has been shown to adopt a coplanar orientation with reference to C_2 – N – C_6 plane due to the delocalization of lone-pair of electrons on ring nitrogen into the carbonyl π-cloud. It results in the change of hybridization of the nitrogen from sp^3 to sp^2. In the chair conformation **CE**, the *p*-anisyl groups at the equatorial orientation alpha to the nitrogen exhibit a severe non-bonded interaction *viz*., $A^{1,3}$ strain, with the coplanar N-C=O function. In order to relieve this $A^{1,3}$ strain**,** an alternate chair form **CA** can be

considered. In this **CA** conformation, the aryl groups are forced to occupy the axial orientation and this conformation would be destabilized by the 1, 3-diaxial interaction between aryl groups as well as aryl groups and C_3-axial methyl group. If both **CE** & **CA** conformations have higher magnitude of destabilizing interactions then other possible conformations may be assumed with boat ring (**B_1-B_6**). In all these boat forms **B_1–B_6**, different destabilizing interactions like $A^{1,3}$ strain (*eg*. **B_2, B_3** & **B_6**), 1, 3-diaxial interactions (*eg*. **B_5**), bond eclipsing interactions, *gauche* interactions, *etc*., would be involved. In such instances, an optimum geometry would be reached by unsymmetrically twisting the ring skeleton**.**

In the chair conformation **CA**, benzylic protons (H_2 & H_6) occupy equatorial orientations and they are in the 'deshielding region' (inplane) of the amide plane. Hence the observed deshielding can be reasonably explained using the Paulsen and Todt's model **[30].** However, the J_{cis} ($J_{6a, 5e}$) and J_{trans} ($J_{6a, 5a}$) coupling constant values for the benzylic proton of C_6 would be expected in the range of 2-4Hz. Also the dihedral angles between H_{6a} & H_{5e} (ϕ_{cis}) and H_{6a} & H_{5a} (ϕ_{trans}) protons are expected around 56-60°. But the observed coupling constant values (compound **2.:** J_{cis} = 6.0 Hz & J_{trans} = 12.0 Hz) and the dihedral angles (ϕ_{cis} = 44° and ϕ_{trans} = 164°) are different and cannot be explained using the conformation **CA**. Hence the possibility of conformation **CA** is also ruled out. In the boat conformations **B_1-B_6**, the observed deshielding of benzylic protons may be explained using the boat forms **B_1, B_2** & **B_5** since in these conformations the benzylic protons are expected to be present in the "deshielding region" of the amide function. The extracted coupling constants and the estimated dihedral angles between H_6 benzylic proton and H_5 (axial & equatorial) protons could be explained only by using boat form **B1**. In addition, the magnitude of coupling constants (J_{cis} = 6.0 Hz & J_{trans} = 12.0 Hz) and the dihedral angles (ϕ_{cis} = 44° & ϕ_{trans} 164°) eliminate the possibility of an equilibrium between two boat conformations **B_1** & **B_2**.

At least, two sets of signals are expected for α-protons and α-carbons if the equilibrium between **B_1** and **B_2** is slow when compared to NMR time scale. However, in these compounds **2-5**, only isochronous proton and carbon signals have been observed which indicate a fast equilibrium. In the N-C=O function, the conjugation of nitrogen lone pair with >C=O creates a partial double bond character at N-C bond and leads to restricted rotation around this bond which in turn is responsible for the fast rotational equilibrium (since the double bond character is less in these compounds **2-5** when compared to *N*-NO system). The observed coupling constants and the dihedral angles cannot be explained even

if a fast equilibrium is assumed between **B_1** & **B_2**. The J_{trans} values are different for the *N*-acyl compounds **2-5** (for **2**: 12.0 Hz; **3** & **5**: 10.0 Hz & **4** : 10.5 Hz) when compared to the other reported *N*-acyl systems (J_{trans}= 6-8 Hz). The higher value of J_{trans} (10-12 Hz) and ϕ_{trans} (158-164^o) would not have been possible if the equilibrium is assumed between **B_1** & **B_2**. Hence the possibility of an equilibrium between **B_1** and **B_2** is eliminated and for all these *N*-acyl compounds **2-5** the rotational equilibrium with **B_1** conformation is assumed (**Fig. 9**).

In this **B_1** conformation, the C_6 benzylic proton occupies axial position. It makes a *trans* angle around 160^o [H_{6a}–C_6–C_5–H_{5a}] and a *cis* angle around 45^o [H_{6a}–C_6– C_5–H_{5e}] with C_5 axial and equatorial protons, respectively. Hence, the observed coupling constant values for all the *N*-acyl compounds **2-5** (J_{trans} = 10-12 Hz & J_{cis} = 6.0 – 6.5 Hz, **Table 4**) .and the estimated dihedral angles using DAERM (ϕ_{trans} = 158-164^o & ϕ_{cis} = 38-44^o) can be explained using the boat conformation **B_1**. In all these *N*-acyl compounds **2-5,** the magnitude of desheilding of H_2 benzylic protons are more compared to H_6 benzylic protons [for *eg*. **2** : $\Delta\delta$ of H_2 = +2.72 ; H_6 = +1.05]. In the boat conformation **B_1**, there exists *gauche* interaction between C_2-Ar group and the equatorial methyl group at C_3 **(Fig.10)**. In order to avoid this interaction, a slight twist along N-C_2-C_3 may takes place which brings the H_2 proton well into the deshielding region of the amide plane. Hence, the H_2 protons are more deshielded than H_6 protons in all these *N*-acyl compounds, when compared to the parent amine **1,** (**Table 5**).

Support for the above speculation is obtained from the magnitude of shielding of carbons observed in the ^{13}C NMR spectrum (**Table 6**). For example, in compound **2**, the C_2 & C_6 carbons are shielded by -7.59 and -3.76 ppm, respectively, compared with that of the parent piperidin-4-one **1**. It again confirms that the carbonyl group is coplanar to the C_2-N-C_6 plane of the piperidine ring causing *gamma*-eclipsing interaction between C-O and N-Cα bonds. Hence, the shielding of α-carbons (C_2 & C_6) is ascribed to the *gamma* eclipsing interaction between N_1-C_2 / N_1-C_6 bond with C-O bond. The magnitude of shielding of C_2 benzylic carbon ($\Delta\delta$ = -7.59 ppm) is more than the C_6 benzylic carbon ($\Delta\delta$ = -3.76 ppm). Due to *gauche* interaction between C_2-Ar & C_3-Me groups **(Fig.10),** the ring undergoes a slight twist along N-C_2-C_3 bonds. The slight twisting along N-C_2-C_3 bonds would reduce the dihedral angle between N-C-O and C-N-C_2 planes and the γ -eclipsing interaction between the C-O & N-C_2 bonds may be more compared to that of C-O & N-C_6 bonds. The shielding of β - carbons is attributed to the γ-*anti* effect induced at the β-carbon by the N-C bond. Hence, based on the coupling constants, chemical shifts and estimated dihedral angles, it is

concluded that the *N*-acyl piperidin-4-ones **2-5** prefer the *N*-CO rotational equilibrium between $\mathbf{B_1}$ conformations [$\mathbf{B_1}$ **(I)** & $\mathbf{B_1}$ **(II)**] with a slight twist along N-C_2-C_3 bonds and C_2 & C_5 in prow and stern positions with a coplanar N-C=O group (**Fig. 9**).

4. Antibacterial activity of compounds 1-5

The biological activity against the synthetic test compounds of substituted piperidin-4-ones **1-5** is assessed using bacterial isolates that are obtained from processed clinical samples. Anti-bacterial activity of the above test compounds is determined against the *pseudomonas sp*. and *salmonella sp*. The minimum inhibitory concentration (MIC) for compounds **1-5** has been assessed by two fold serial dilution methods. The results are compared with standard drugs *viz.,* chloramphenicol and gentamycin (**Tables 7 & 8**). The results indicate that all the compounds **1-5** possess a broad spectrum of activity against the tested microorganisms even at 6.25 μg/ml. Compounds **1-5** exhibit superior activity against *pseudomonas species* and significant activity against *salmonella species* when compared to the above standard drugs. Compound **4** containing dichloroacetyl group shows superior antibacterial activity against *pseudomonas* when compared to all other groups.

5. Antioxidant

The DPPH radicals scavenging method, ABTS assay methods and Superoxide radicals (O_2^-) scavenging activity are the most common tools to inspect the antioxidant capacity of the specific compounds. The synthesized compounds **1-5** interact with the above free radicals, inhibit the oxidation and there by exhibiting a certain degree of radical scavenging activity. The results of the compounds **1-5** are compared with standard Rutin and BHT and are presented in **Table 9**. The values of IC_{50}, the effective concentration at which 50% of the radicals are scavenged, are tested to evaluate the antioxidant activities. Generally, a lower IC_{50} value demonstrates greater antioxidant activity. With ABTS radicals, the compound **4** is found to possess a better antioxidant activity, compounds **1, 3 & 5** show a moderate activity and compound **2** shows a very poor activity when compared to the standards. In the DPPH assay, the antioxidant activity of all the compounds **1-5** is found to be moderate when compared to the standards. With superoxide assay, the compound **5** shows a better activity, compounds **2-4** show a moderate activity, and compound **1** shows poor activity when compared to the standards. The ABTS, DPPH and superoxide scavenging abilities are found to be in the order of **4>1>5>3>2, 4>2>3>5>1** and **5>3>2>4>1,** respectively.

6. Molecular Docking Studies

6.1 Binding mode of *r*-2,*c*-6-bis(4-methoxyphenyl)-*c*-3,*t*-3-dimethyl-piperidin-4-one (1) into *CHK1*

Docking simulation of **1** into *CHK1* results in the formation of single hydrogen bond interaction with bond distance of 2.11Å and it is observed that side chain hydrogen atom of positive charged residue of ASN 59 interacts with oxygen atom of **1**. The Glide Score and Glide Energy values for piperidin-4-one **1** are observed to be -5.710 kcal/mol and - 47.773 kcal/mol (**Table-10**). Furthermore, a number of hydrophobic interactions (LEU 82, LEU 137, PHE 149, ALA 36 VAL 23, TYR 86 & CYS 87) are found between piperidin-4-one **1** ***into*** *CHK1* protein **(Fig.11).**

6.2 Binding mode of *N*-phenyl carbamoyl-*r*-2, *c*-6-bis(4-methoxyphenyl)-*c*-3, *t*-3-dimethylpiperidin-4-one(2) into *CHK1*

Docking simulation of **2** within the active site of the checkpoint kinase1 has been analyzed. The Glide Score and Glide Energy values for **2** are observed as -2.473 kcal/mol and -31.04 kcal/mol, respectively (**Table-10**). Upon examining the docking features between compound **2** and *CHK1,* two hydrogen bond interactions are found to be present. First one is the side chain hydrogen atom of the positive charged residue of LYS 38 and it is well interacted with oxygen atom of the compound **2** (with bond length 2.35Å). The second one is the backbone hydrogen atom of the negative charged residue of GLU 17 which is strongly interacted with oxygen atom of the compound **2** (with bond distance 2.18Å). Furthermore, a number of hydrophobic interactions (LEU 82, LEU 84,PHE 149, ALA 36 VAL 23, LEU 137 & LEU 15) are found between compound **2** into *CHK1* protein **(Figs.11&12)**.

6.3 Binding mode of *N*-chloroacetyl-*r*-2, *c*-6-bis(4-methoxyphenyl)-*c*-3, *t*-3-dimethyl-piperidin-4-one (3) into *CHK1*

Docking simulation of compound **3** within the active site of the checkpoint kinase1 has been analyzed. The Glide Score and Glide Energy values for compound **3** are -4.42 kcal/mol and - 53.504 kcal/mol, respectively. On examination of docking features between compound **3** and checkpoint kinase1, only one hydrogen bond interaction is found to be present. The hydrogen atom of the CYS 87 is well interacted with oxygen atom of the compound **3**. Furthermore, a number of hydrophobic interactions (TYR 86, ALA 36, TYR 86, LEU 84, VAL 23, VAL 68, TYR 20 & LEU 15) are found between compound **3** into ***CHK1*** protein **(Fig. 12).**

6.4 Binding mode of *N*-dichloroacetyl-*r*-2, *c*-6-bis(4-methoxyphenyl)-*c*-3, *t*-3-dimethylpiperidin-4-one(4) into *CHK1*

Docking simulation of compound **4** within the active site of the checkpoint kinase1 has been analyzed. The Glide Score and Glide Energy values for compound **4** are observed to be -2.840 kcal/mol and -21.835 kcal/mol. Examination of docking features between compound **4** and checkpoint kinase1 reveals only one hydrogen bond interaction between compound **4** into ***CHK1***. Furthermore, a number of hydrophobic interactions (LEU 151, TYR 86, ALA 36,VAL 23 & LEU 15) are found between compound **4** into ***CHK1*** protein **(Fig.12).**

6.5 Binding mode of *N*-morpholinoacetyl-*r*-2, *c*-6-bis(4-methoxyphenyl)-*c*-3, *t*-3-dimethylpiperidin-4-one(5) into *CHK1*

Docking simulation of compound **5** within the active site of the checkpoint kinase1 has been analyzed. The Glide Score and Glide Energy values for compound **5** are observed to be -3.892 kcal/mol and -16.751 kcal/mol **(Fig. 11**). On examination of docking features between compound **5** and checkpoint kinase1, only one hydrogen bond interaction is found to be present. The side chain hydrogen atom of the positive charged residue of LYS 38 is well interacted with oxygen atom of the compound **5** with bond distance of 2.46Å. Furthermore, a number of hydrophobic interactions (LEU 137, LEU 15, CYS 87, ALA 36, VAL 23, LEU 84, VAL 68, ILE 146, LEU 62, PHE 149 & TYR 20) are found between compound **5** into ***CHK1*** protein **(Figs. 11 & 12)**. The Glide Score and Glide Energy for all compounds **1-5** are given in **Table. 9**.

Conclusion

N-Phenylcarbamoyl, *N*-chloroacetyl, *N*-dichloroacetyl and *N*-morpholinoacetyl derivatives **2-5** of *r*-2, *c*-6-bis(4-methoxyphenyl)-*c*-3,*t*-3-dimethylpiperidin-4-one (**1**) have been synthesized and characterized. The preferred conformation of these compounds **1-5** have been determined using IR spectra and ^{1}H, ^{13}C, DEPT & 2D (^{1}H, ^{1}H-COSY & ^{1}H-^{13}C-HETCOR) NMR spectra. The mass spectra for all the compounds have been recorded to confirm the structure. On the basis of the coupling constants, chemical shifts and estimated dihedral angles it is found that the *N*-acyl piperidin-4-ones **2-5** prefer to exist in a distorted boat conformation $\mathbf{B_1}$ **(** with C_2 and C_5 in prow and stern positions) with coplanar orientation of *N*-C=O moiety. The existence of a fast N-CO rotational equilibrium between the distorted boat conformations $\mathbf{B_1}$ has also been observed. The antibacterial activity of substituted piperidin-4-ones **1-5** is assessed against the bacterial isolates that were obtained from processed clinical samples. Anti-bacterial activity of the above test compounds is

determined against *pseudomonas sp*. and *salmonella sp*. The results clearly show that all the five compounds demonstrate a significant anti-bacterial activity. The results of antioxidant studies show that most of the compounds posses moderate activity when compared to the standards Rutin and BHT. The compounds **1-5** have been docked with the structure of ***CHK1*** and the results demonstrate that all the compounds show good binding affinity.

Acknowledgement

We thank Dr. T. Viswanathan for antibacterial activity studies.

References

[1] J. R. Dimmock,; V. K. Arora, S. L .Wonko, N. W. Hamon, J. W. Quail, , Z. Jia, R.C. Warrington, W. D. Fang, J. S. Lee, *Drug Des. Deliv.* 6 (1990) 183-194.

[2] S. Manikandan, S. Dhanuskodi, *Spectrochim. Acta. Part A.* 67 (2007) 160–165.

[3] U. Das, J. Molnr, Z. Barth, Z. Bata, J. R. Dimmock, *Bioorg. Med. Chem. Lett*. 18 (2008), 3484–3487.

[4] S. Das, U. Das, B. Bandy, D. K. J. Gorecki, J. R. Dimmock, *Pharmazie* 63 (2008), 827–829.

[5] Bingsen Zhou, Shuya Hu, Yun Yen, *Bioorg. Med. Chem. Lett.* 18 (2008) 6248–6250.

[6] R. V. Perumal, M. Adiraj, P. Shanmugapandiyan, *Indian Drugs*, *38* (2001), 156-159.

[7] G. Aridoss, S. Balasubramanian , P. Parthiban, S. Kabilan, *Eur. J. Med. Chem.* 41 (2006) 268–275.

[8] S. Sethuvasan, P. Sugumar, V. Maheshwaran, M.N. Ponnuswamy, S. Ponnuswamy, *J. Mol. Struc.*1116 (2016)188-199.

[9] Y. Zhang, T. Hunter *Int. J. Cancer,* 134 (2014) 1013–1023.

[10] C. Ramalingan, S. Balasubramanian, S. Kabilan, M.Vasudevan, Eur. *J. Med. Chem,* 39 (2004) 527–533.

[11] J. Jayabharathi A. Thangamani M. Padmavathy B. Krishnakumar, *Med. Chem. Res.* 15 (2007) 431–442.

[12] G. Aridoss., S. Balasubramanian., P. Parthiban., S. Kabilan., *Eur. J. Med. Chem* 42 (2007) 851-860.

[13] P. Sakthivel, S. Ponnuswamy, *J. Mol. Struct*. 1074 (2014) 349–358.

[14] A. Akila, P. Jeganathan, S. Ponnuswamy, *J. Mol. Struc.* 1120 (2016) 187-195.

[15] S. Ponnuswamy, S. Sethuvasan, K. Thirunavukarasu, *J. Mol. Struct*. 1089 (2015) 86-94.

[16] F. Johnson, S. K. Malhotra, *J. Am. Chem. Soc*. 87 (1965) 5492.

[17] K. N. Slessor, A.S. Tracey. *Can. J. Chem*. 50 (1972) 1594.

[18] S. Ponnuswamy, V. Mohanraj, P. Gayathri, A. Thiruvalluvar, R. J. Butcher, *Acta Cryst*. E64 (2008) o2328.

[19] C.R. Noller, V. Baliah, *J. Am. Chem. Soc*. 70 (1948) 3853-3855.

[20] G. Aridoss, S. Amirthaganesan, M.S. Kim, J.T. Kim, Yeon Tae Jeong, *Eur. J. Med. Chem*. 44 (2009) 4199-4210.

[21] M.S. Blois, Antioxidant determinations by the use of a stable free radical. *Nature*, 26 (1958) 1199-1200.

[22] Re, R. Pellegrini, N. Proteggente, A. Pannala, A. Yang, M. Rice-Evans, C. *Free Radical Biology & Medicine,* 26 (1999) 1231-1237.

[23] C. Beauchamp, I. Fridovich, *Analytical Biochemistry*, 44 (1971) 276-287.

[24] P. Chen, C. Luo. Y.Deng, K. Reyan, J.Register, S. Margosiak, A. Tempezyk-Russell, B. Nguyen,P.Myers. K. Lundgren, C.C. Kan, P.M.O'Connor, *Cell*, 100 (2000) 681-92

[25] T. Ravindran, R. Jeyaraman, R. W. Murray, M. Singh, *J. Org. Chem.* 56 (1991) 4833-4840.

[26] S. Ponnuswamy, M. Venkatraj, R. Jeyaraman, M Suresh Kumar, D. Kumaran, M. N Ponnuswamy, *Ind. J. Chem.* 41B (2002) 614-627.

[27] S. Ponnuswamy, R. Kayalvizhi, M. Jamesh, J. Uma Maheswari, M. Thenmozhi, M.N. Ponnuswamy, *J. Mol. Struct*. 1120 (2016) 70-78.

[28] F. Bholmann, Angew. Chem. 69 (1957) 641.

[29] R. Jeyaraman, T. Ravindran, M. Sujatha & M. Venkatraj, *Indian J. Chem*. 38B (1999) 52-55.

[30] H. Paulsen, K. Todt, Angew. *Chem. Int. Ed. Engl.* 5 (1966) 899-900.

Figure captions:

Fig.1: Delocalisation along N-X=Y function.

Fig. 2: Allylic strain or $A^{1,3}$ strain.

Fig. 3: ^{1}H NMR spectrum of compound **2**

Fig. 4: ^{13}C NMR spectrum of compound **2**

Fig. 5: DEPT 135 spectrum of compound **2**

Fig. 6: ^{1}H-^{1}H COSY spectrum of compound **2**

Fig. 7: HSQC spectrum of compound **2**

Fig. 8: Possible conformations of *N*-acylpiperidin-4-ones **2-5**.

Fig. 9: Conformational equilibrium in *N*-acyl piperidin-4-ones **2-5**

Fig. 10: *Gauche* interacting between C_2-Ar and C_3-Me group

Fig. 11: Docked structure of target protein CHK1 with compound **1** and **2**

Fig. 12: Hydrophobic interactions found between compounds **2-5** and CHK1

.

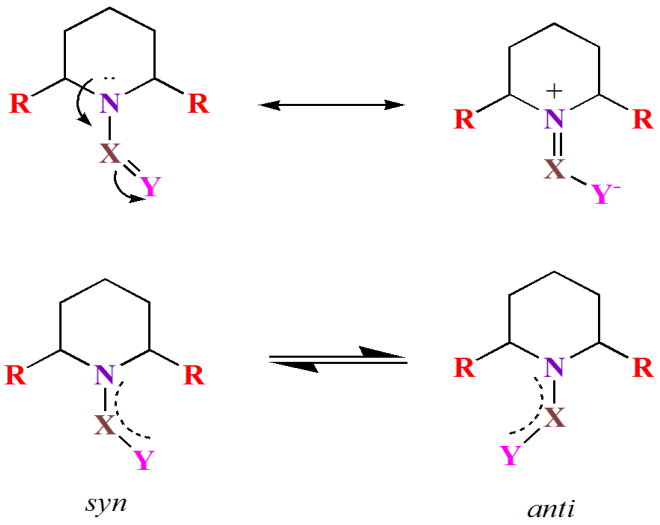

Fig. 1

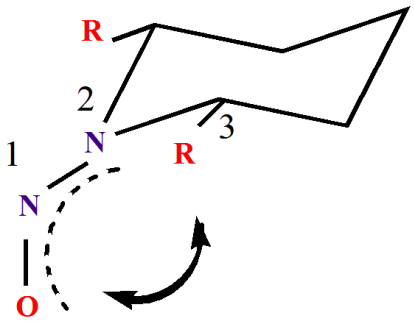

R = alkyl (or) aryl

Fig. 2

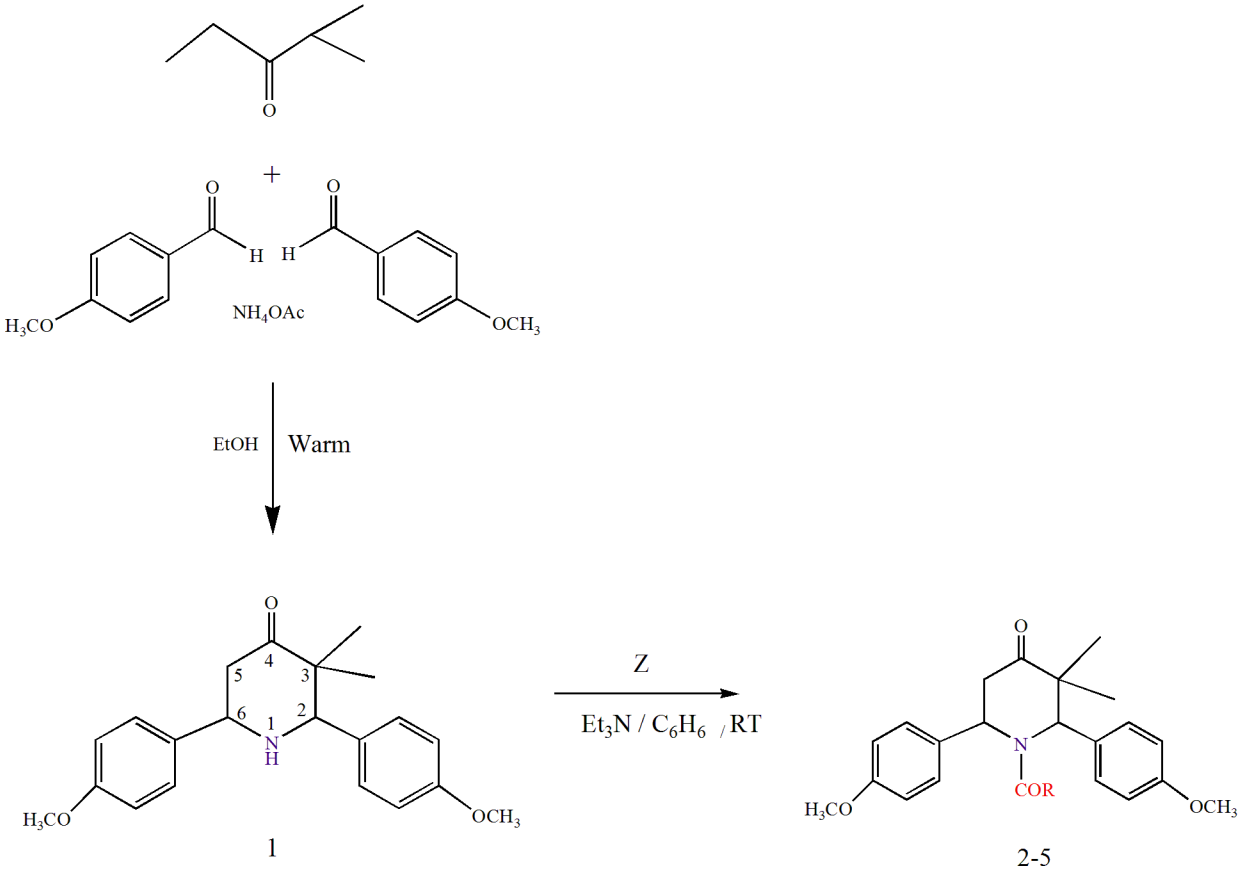

Compound	Z	R
2	C_6H_5NCO	$-NHC_6H_5$
3	$ClCOCH_2Cl$	$-CH_2Cl$
4	$ClCOCHCl_2$	$-CHCl_2$
5	Morpholine	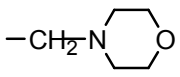

Scheme-1

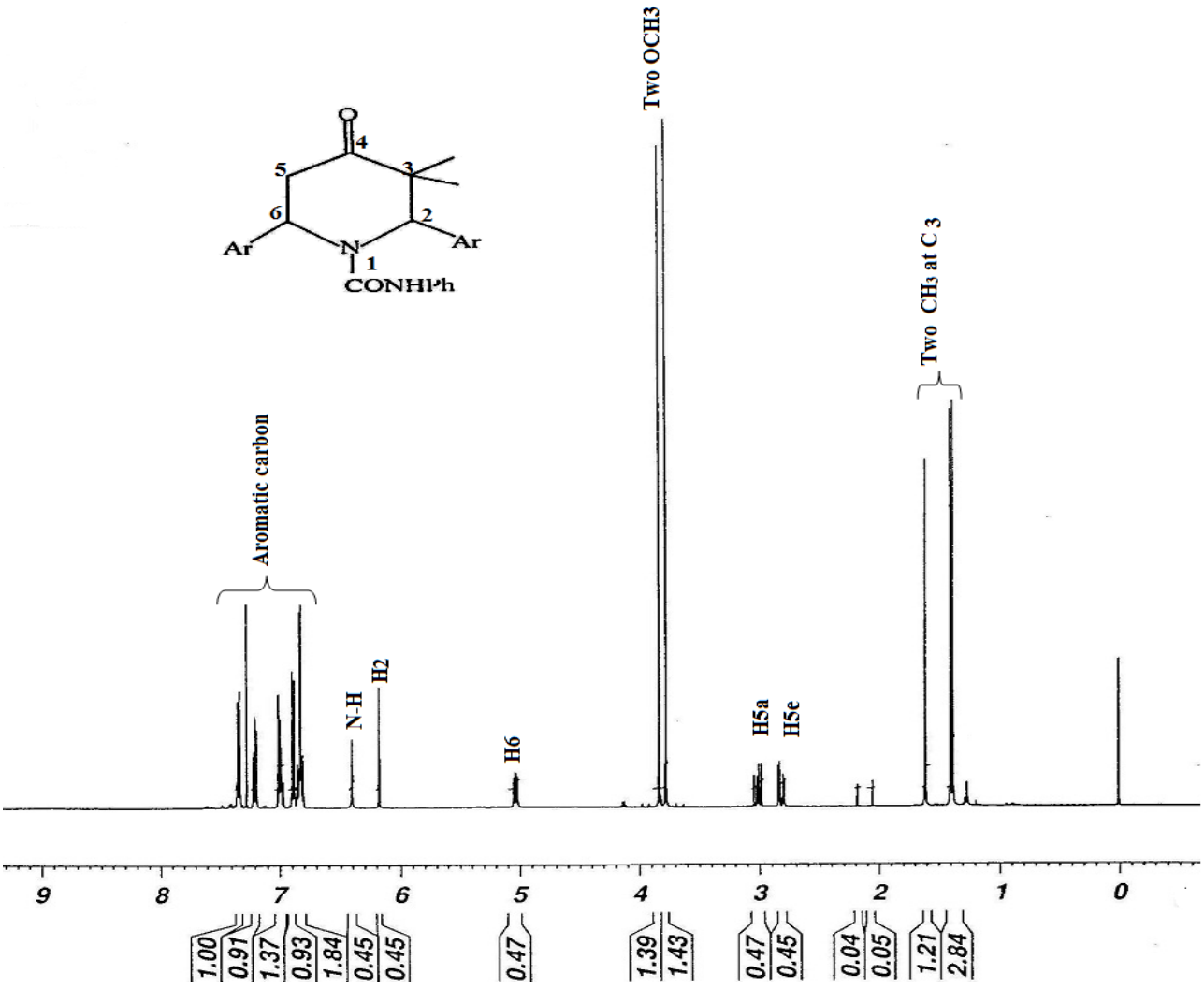

Fig. 3: ^{1}H NMR spectrum of compound **2**

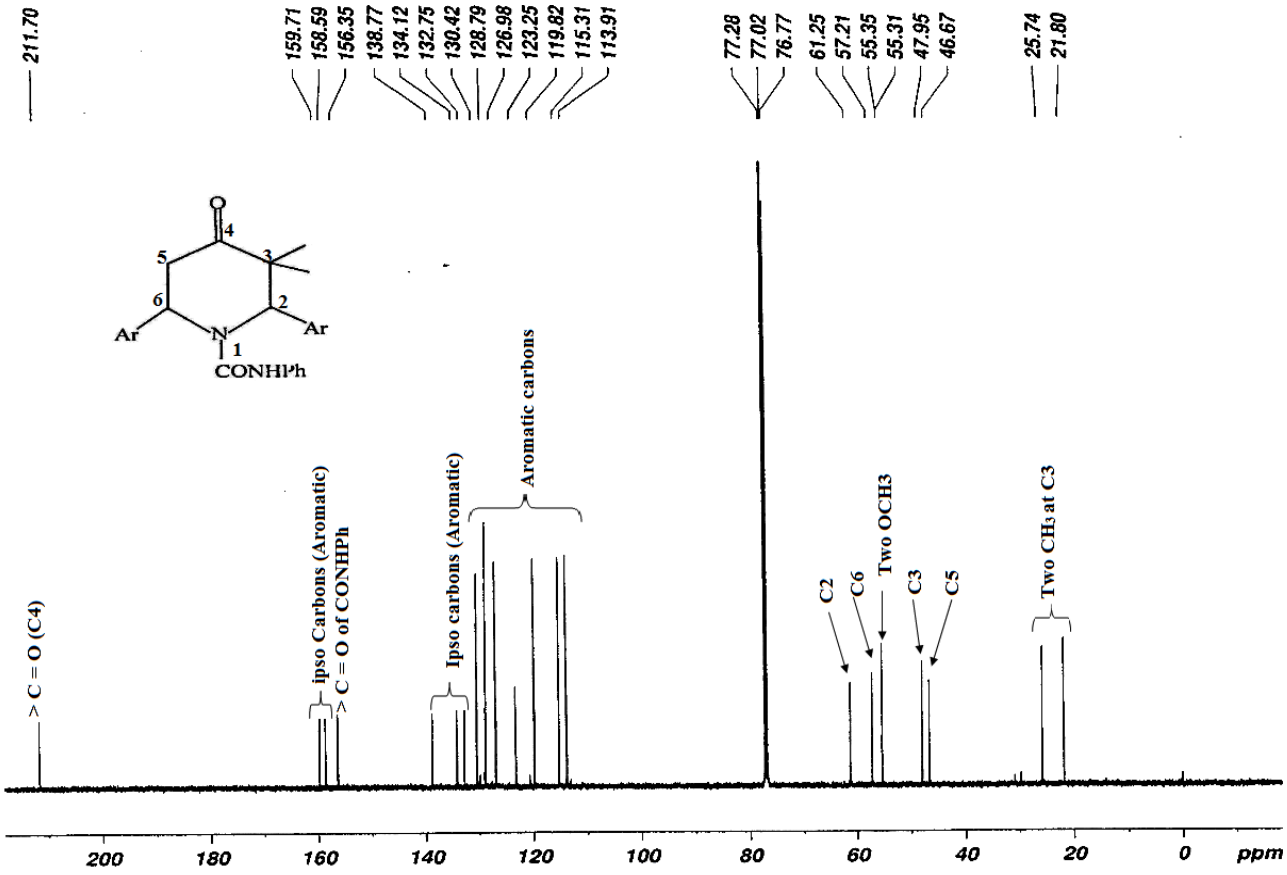

Fig. 4: ^{13}C NMR spectrum of compound **2**

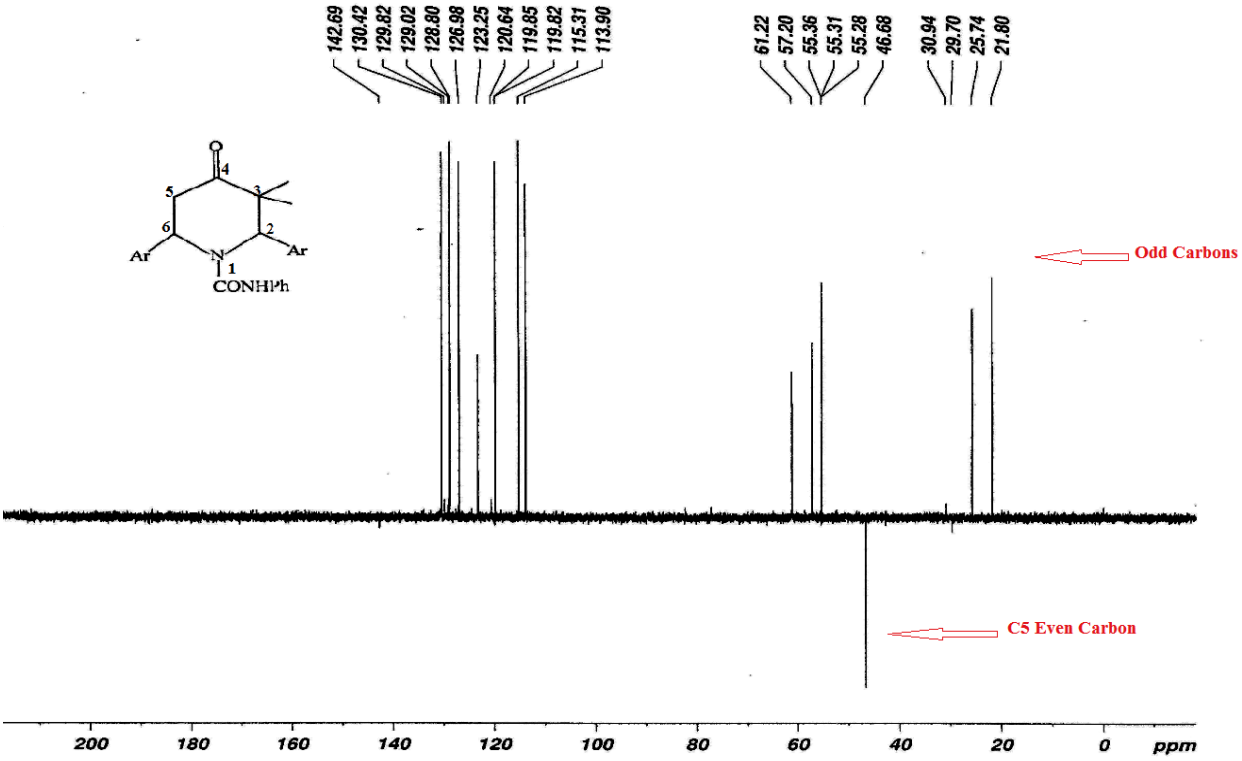

Fig. 5: DEPT 135 spectrum of compound **2**

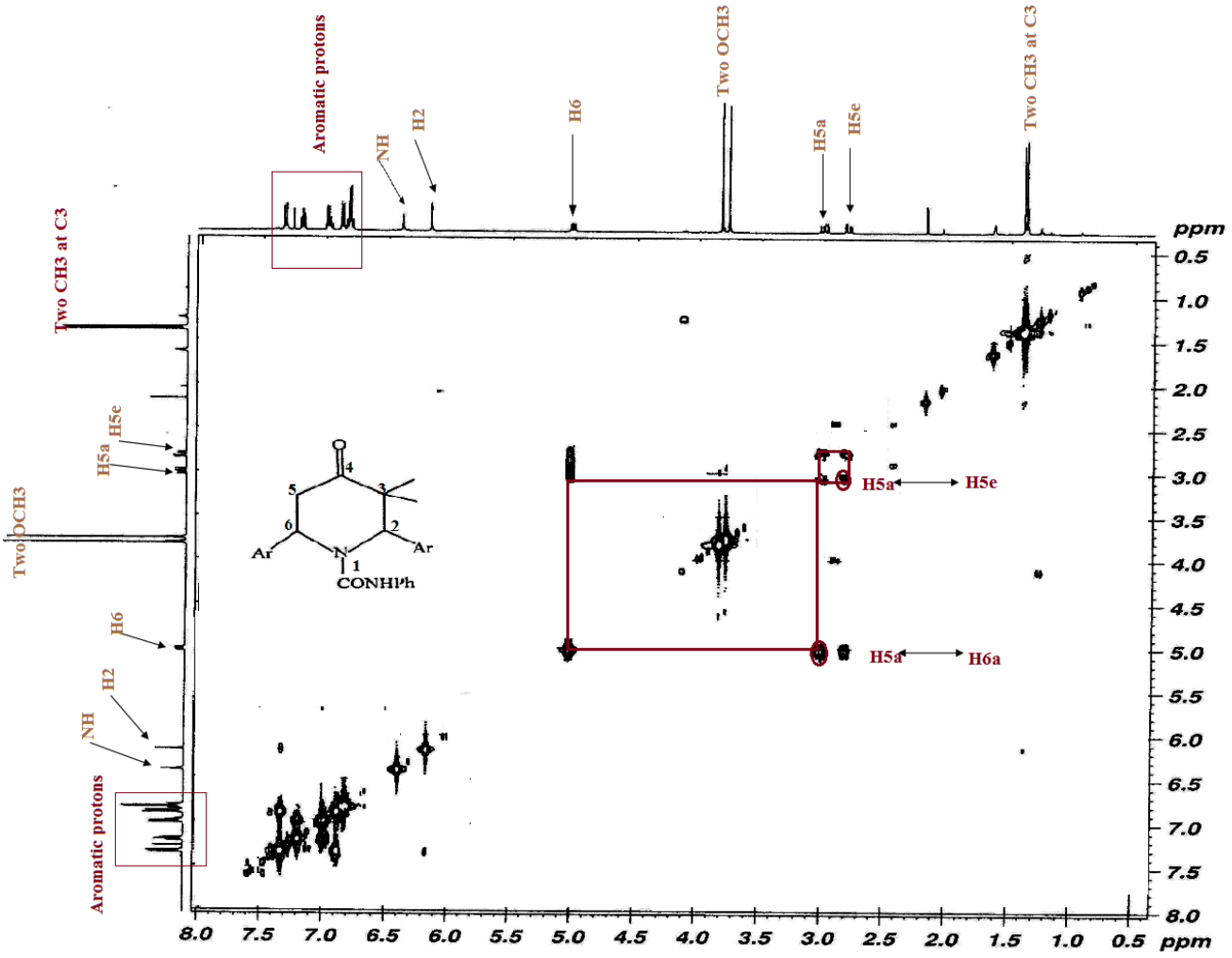

Fig. 6: ^{1}H-^{1}H COSY spectrum of compound **2**

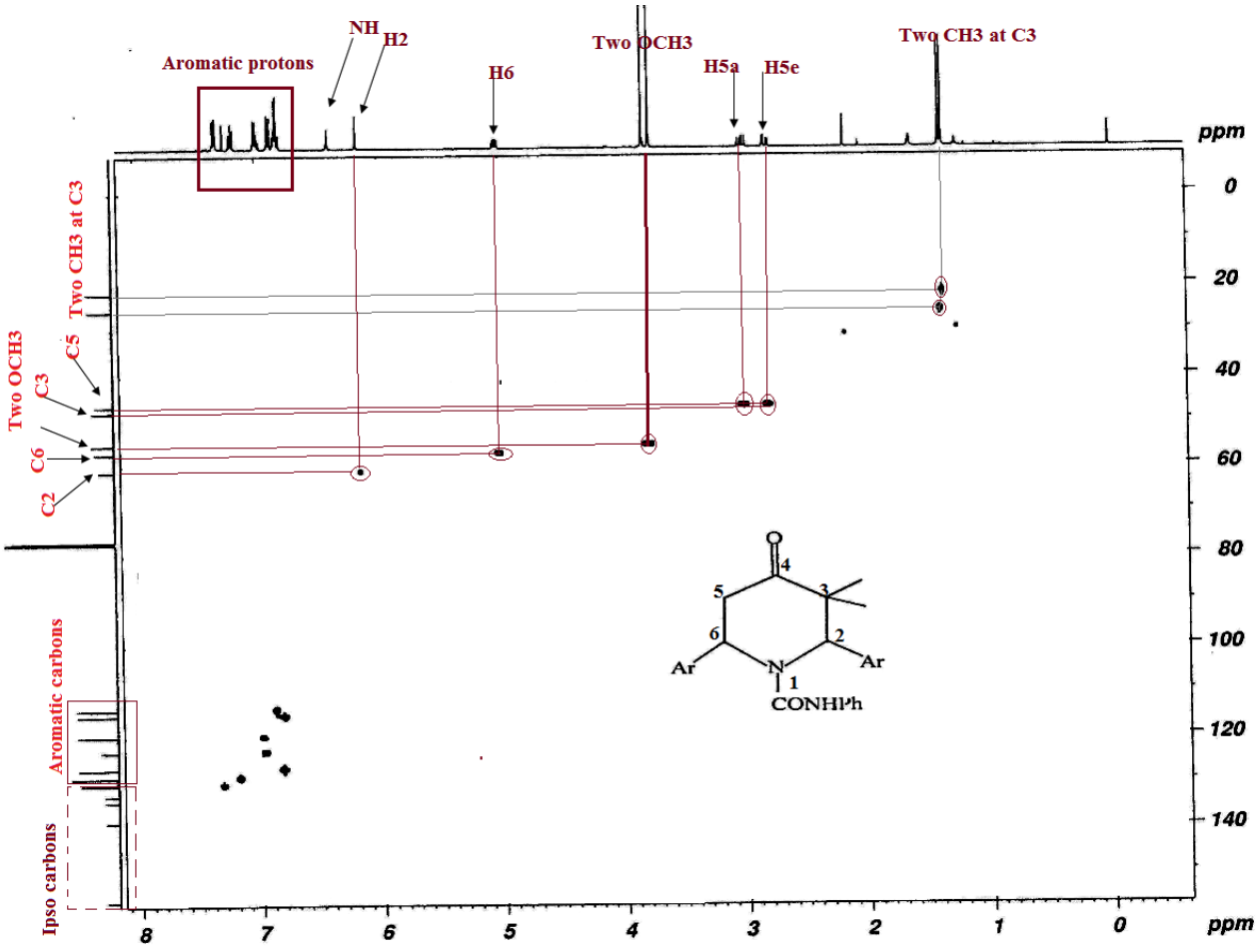

Fig. 7: HSQC spectrum of compound **2**

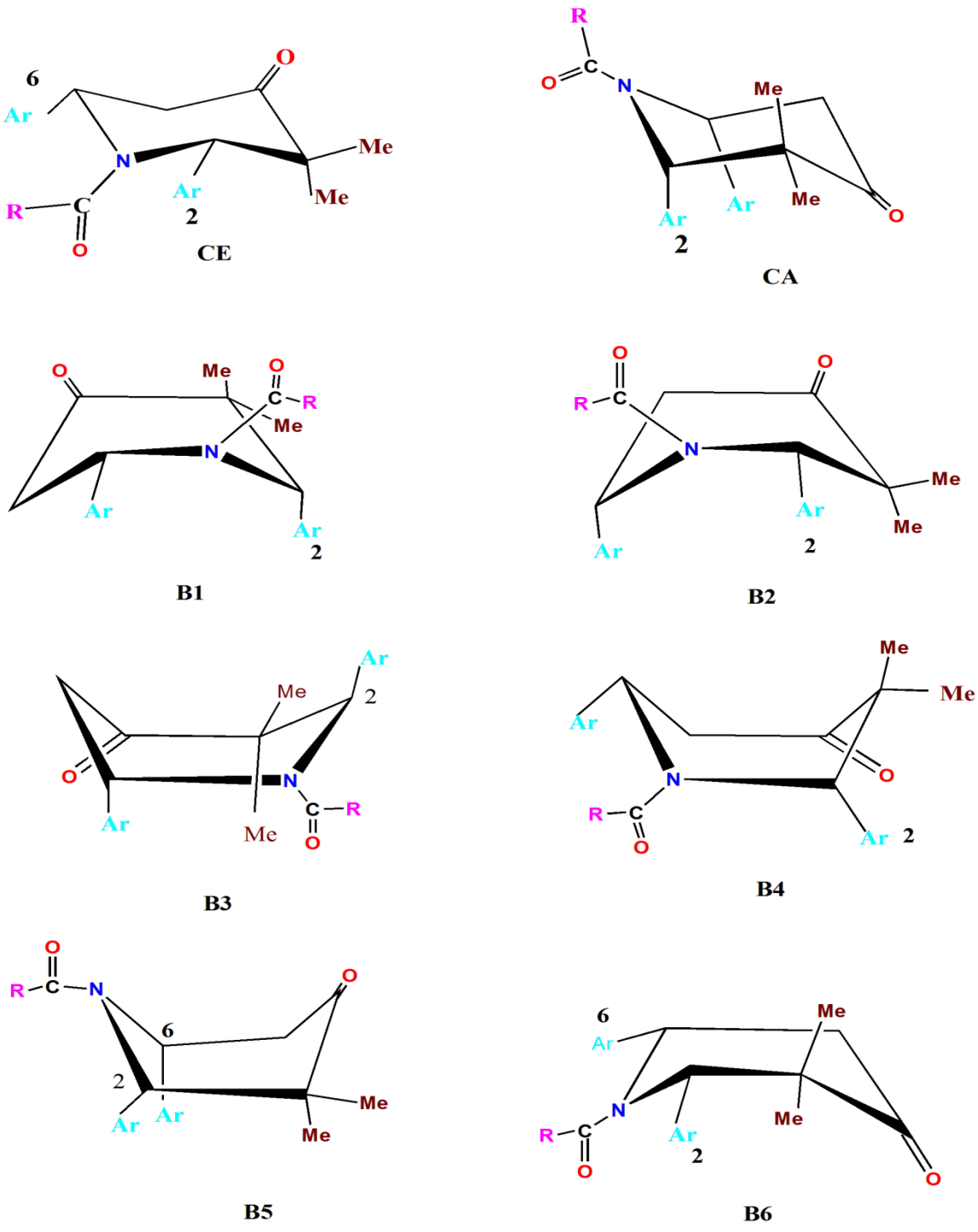

Fig. 8: Possible conformations of *N*-acylpiperidin-4-ones **2-5**. Ar = p-anisyl

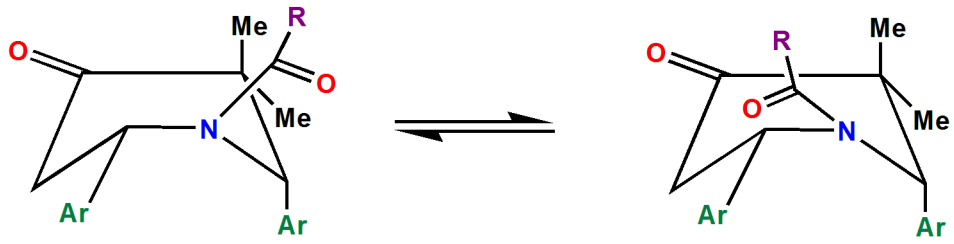

B_1(I) B_1(II)

Fig. 9: Conformational equilibrium in *N*-acyl piperidin-4-ones **2-5**

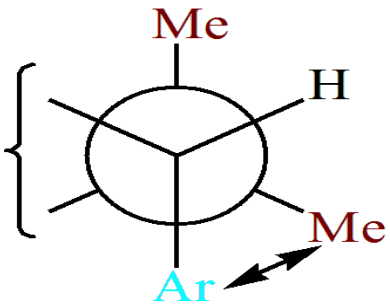

Fig. 10: *Gauche* interacting between C_2-Ar and C_3-Me groups

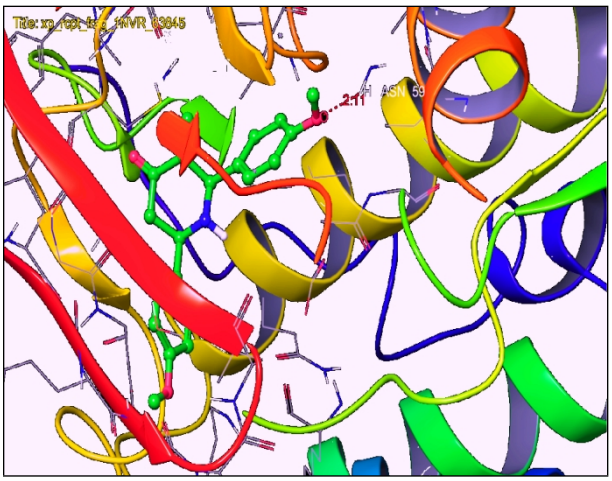

Compound 1

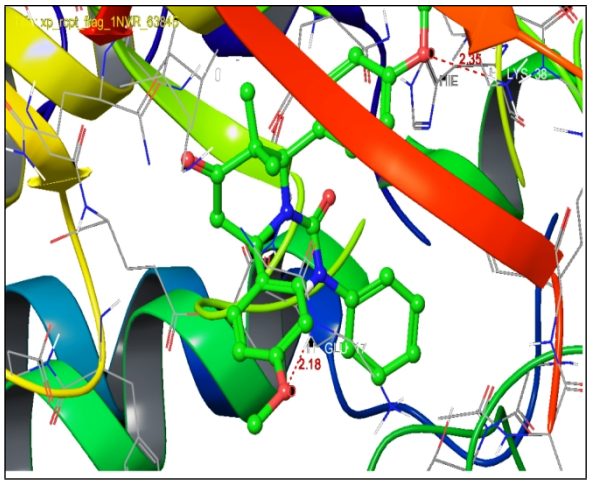

Compound 2

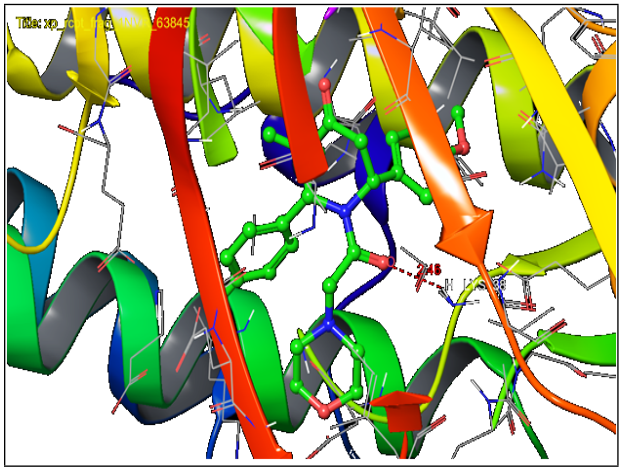

Compound 5

Fig.11: Docked structure of target protein CHK1 with compounds **1**, **2 and 5**

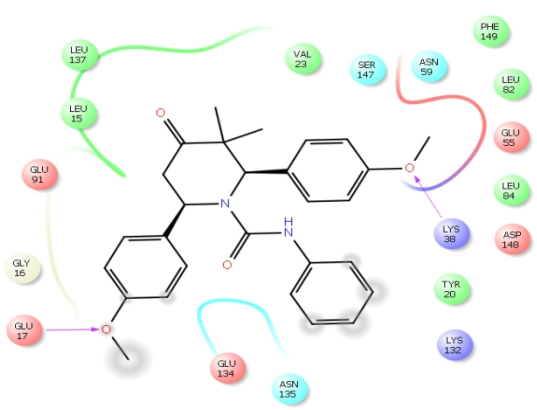

2

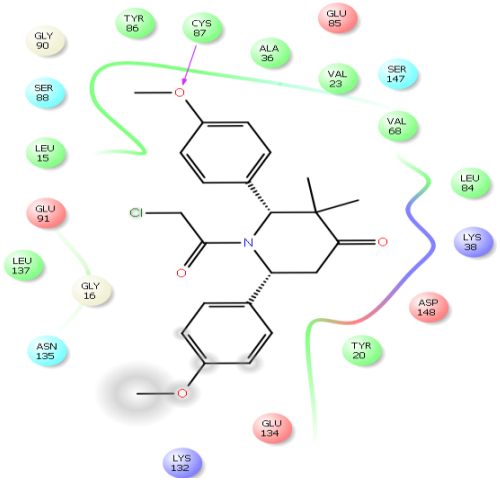

3

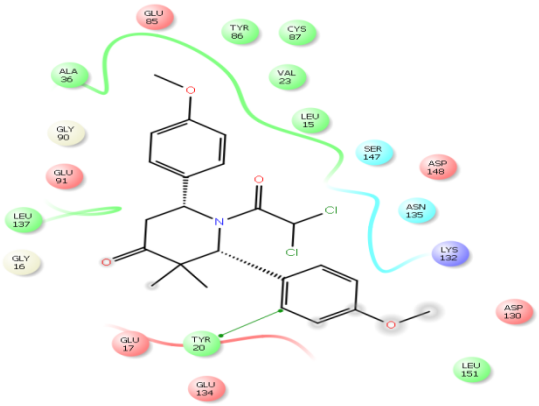

4

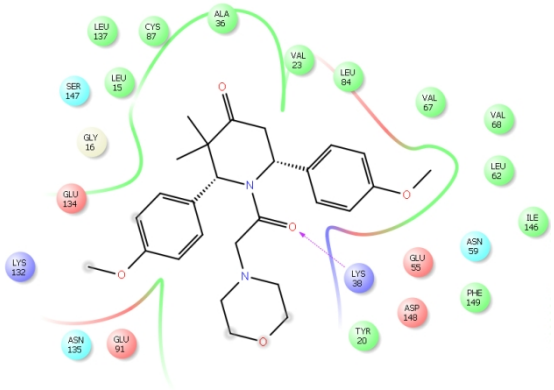

5

Fig.12: Hydrophobic interactions found between compounds **2-5** and CHK1.

Table.1: Analytical data of compounds 1 - 5

Compounds	Molecular formula	Molecular weight	Yield %	M.P (^{o}C)
1	$C_{21}H_{26}NO_3$	339.89	72.4	70-72
2	$C_{28}H_{31}N_2O_4$	459.01	56.0	170-172
3	$C_{23}H_{27}NO_4Cl$	415.54	64.0	91-93
4	$C_{23}H_{26}NO_4Cl_2$	450.03	65.0	102-106
5	$C_{27}H_{35}N_2O_5$	467.00	58.0	81-83

Table.2. Spectral data of the compounds 1-6

Compds	IR(KBr) cm^{-1}	^{1}H NMR($CDCl_3$, δ ppm)	^{13}C NMR($CDCl_3$, δ ppm)	Mass (M^+) m/z
1	3265(N-H Str), 1703(>C=0 Str).	0.94 (S,3H,CH_3 at C_3), 1.19(s,3H, CH_3atC_3), 1.90(Broads, exchangeable with D_2O), NH, 2.45 (dd,1H,H_5-equatorial), 2.90 (Unsym, t, 1H, H_5 axial) ,3.76 (s, 1H, H_2 axial), 3.81(s, 6H, two. OCH_3) 3.99 (dd, 1H, H_6 axial), 6.85-7.43 (m,8H Aromatic).	19.9 CH_3 atC_3), 20.4 (CH_3 at C_3), 47.3 (C_5), 50 (C_3) 55.2 and 55.1 (twoOCH3), 61.0(C_6),68.8 (C_2),129.7,127.6, 113.9, 113.0 (AromaticCarbons) 159.0, 135.4, 131.4 (Aromatic (*ipso*) Carbons, 213.2 C4>=O	**339**
2	3301 (>NH of CONHPh), 1651(>C=0 of CONHPh) 1705 (ring >C=0 str)	1.40 (S,3H,CH_3 at C_3),1.38(S,3H, CH_3 at C_3), 2.82 (dd, 1H,H_5 equatorial), 3.02 (dd,1H,H_5 axial), 3.84 (S,3H) & 3.78 (S,3H, Two OCH_3), 5.04 (dd,1H) H_6.6.18 (S, 1H). H_2, 6.41 (br.S,1H) NH, 6.81-7.35(m,13 H) Aromatic.	21.80 & 25.74 (Two CH_3 atC_3), 46.67 (C_5), 47.95 (C_3), 55.35 & 55.31(Two OCH_3), 57.21(C_6), 61.25C_2, 130.42, 129.79, 126.98, 123.25, 119.82, 115.31, 113.91 (Aromatic Carbons), 159.71, 158.59, 138.77, 134.12, 132.75, (Ipso Carbons) (Aromatic), 156.35 >C = 0 of CONHPh, 211.70 > C = 0 (C_4)	**458**
3	1720 (ring >C=0 str) 1639(>C=O of $COCH_2Cl$)	1.36 (S,3H) and 1.29 (S,3H, Two CH_3 at C_3), 2.92 (dd, 1H,H_5 equatorial), 3.02 (dd, 1H, H 5 axial), 3.76 (mingled with OCH_3, 1H, H_B of –$COCH_2Cl$), 3.79(S,3H) & 3.70 (S, 3H, Two OCH_3), 3.94 (d,1H, H_A of-$COCH_2Cl$) ; 5.38(Unsym t,1H, H_6 axial), 6.09 (br-S,1H) H_2, 6.61 – 7.27 (m,8H) Aromatic	21.60 & 26.01 (Two CH_3 at C_3), 42.53 (CH_2 Cl of Chloroacetyl group), 45.38 (C_5), 47.67(C_3), 55.26 & 55.24 (Two OCH_3) 56.81(C_6), 62.32(C_2), 159.02, 130.69, 128.3, 126.38, 114.70, 113.83, 113.53 (Aromatic Carbons),134.26, 130.84 ipso Carbons (aromatic), 168.25 >C=0 of chloroacetyl group at N, 211.01 C_4(>C=0)	**415**
4	1719 (ring >C=0Str), 1657(>C=O of $COCHCl_2$)	1.37 (S,3H & 1.31 (S,3H, Two CH_3 at C_3), 2.93 (dd, 1H,H_5 equatorial), 3.04 (dd,1H, H_5 axial), 3.80 (S,3H) & 3.73 (S, 3H, Two OCH_3), 5.33 (Unsym, t, 1H) (H_6), 6.07 (S,1H) H_2, 6.09 (S, 1H), $COCHCl_2$ at N_1, 6.65-7.28 (m,8H) Aromatic.	21.63 & 25.90 (Two CH_3 at C_3), 45.51 (C_5), 47.78 (C_3), 63.34 & 55.29 (Two OCH_3), 56.95 (C_6), 65.29 (C_2), 158.98, 130.73, 126.13, 115.09, 114.00 (Aromatic Carbons). 159.34, 133.58, 130.21 (ipso-Carbon (aromatic), 165.83 >C=0 of Dichloroacetyl group at N_1, 210.39 C_4 (>C=0).	**449.85**
5	1712 (ring >C=0str), 1648 (>C=O of >$COCH_2$-Mor)	1.33 (S,3H) & 1.30 (S,3H)- (Two CH_3 atC_3), 2.44(br.s,4H) Two N-CH_2 of morpholine ring, 2.78(br,1H) H_B of $NCOCH_2$-morpholine, 2.90 (dd, 1H) H_{5e}, 3.01(dd, 1H) H_{5a}, 3.10 (d, 1H) H_a of > N-$COCH_2$-morpholine. 3.70-3.76 (m,4H) Two OCH_2 of morpoline ring ,3.8 (S,3H) & 3.72 (S,3H) Two OCH_3,5.66 (Unsym t,1H) H_6, 6.16(br,S,1H) H_2, 6.60-7.37 (m,8H) Aromatic.	21.54 & 26.04 Two CH_3 at C_3, 30.92 C_5, 47.59 C, 53.99 Two N-CH_3 of morpoline ring, 55.26 & 55.23 Two OCH_3, 56.22, C_6, 62.36, 66.80 Two OCH_2 of morpoline ring. 158.68, 158.62, 134.80, 131.33, 130.77, 128.33, 126.48, 114.36, 113.68 Aromatic, 170.61 > C=0 at N1, 211.80 C_4(>C=0)	**424**

Table 3: ^{1}H NMR and ^{13}C NMR chemical shifts (δ ppm) of piperidin-4-ones (1-5)

Compounds	H_2	H_{5a}	H_{5e}	H_6	C_2	C_3	C_4	C_5	C_6
1	3.76	2.90	2.45	5.04	68.84	49.95	213.24	47.34	57.21
2	6.18	3.02	2.82	5.04	61.25	47.95	211.70	46.67	57.21
3	6.09	3.02	2.92	5.38	62.32	47.67	211.01	45.38	56.81
4	6.07	3.04	2.93	5.33	65.29	47.78	210.39	45.51	56.95
5	6.16	2.90	2.45	3.99	62.36	47.59	211.80	30.92	56.22

Table 4: Vicinal coupling constants (in Hz) and dihedral angles of the piperidin-4-ones (1-5)

Compounds	$J_{H6,H5a}$	$^{3}J_{H6,\ H5e}$	$^{2}J_{H5a,\ H5e}$	Φ_{cis}	Φ_{trans}
2	12.0	6.0	18.5	44	164
3	10.0	6.5	18.0	38	158
4	10.5	6.5	18.5	39	159
5	10.0	6.5	18.5	38	158
1	12.0	3.0	13.5	57	177

Table 5: Magnitude of deshielding (in ppm) of protons in the *N*-acyl piperidine-4-ones **2-4** from the parent piperidine-4-one **1**

Compound	H_2	H_6	H_{5a}	H_{5e}
2	+2.72	+1.05	+0.12	+0.37
3	+2.33	+1.39	+0.12	+0.47
4	+2.31	+1.34	+0.14	+0.48
3	+2.4	+1.67	+0.11	+0.45

Table 6: ^{13}C NMR chemical shift differences (in ppm) between N-acyl piperdin-4-ones **2-5** and the parent piperdin-4-one **1**

Compound	C_2	C_3	C_4	C_5	C_6
2	-7.59	-2.00	-1.54	-0.67	-3.76
3	-6.52	-2.28	-2.23	-1.96	-4.16
4	-3.55	-2.17	-2.85	-1.83	-4.02
3	-6.48	-2.36	-1.44	-16.42	-4.75

Minimum inhibitory Concentration in ug/ml

Compounds	Dilution at 200 µg	Dilution at 100 µg	Dilution at 50 µg	Dilution at 25 µg	Dilution at 12.5 µg	Dilution at 6.25 µg
1	0.17	0.27	0.43	0.54	0.66	0.75
2	0.02	0.46	0.66	0.74	0.82	0.87
3	0.07	0.80	0.74	0.57	0.81	0.89
4	0.03	0.31	0.82	0.86	0.90	0.97
5	0.12	0.57	0.76	0.81	0.86	0.86
Chloramphenical	-0.08	-0.07	-0.06	-0.02	-0.03	-0.01
Gentamycin	-0.07	-0.03	0.07	0.13	0.17	0.21

Table 7: Biological activity of piperidin-4-ones **1-5** against *Pseudomonas species*

Table 8: Biological activity of piperidin-4-ones **1-5** against *Salmonella species*

Compounds	Dilution at 200 µg	Dilution at 100 µg	Dilution at 50 µg	Dilution at 25 µg	Dilution at 12.5 µg	Dilution at 6.25 µg
1	0.36	0.32	0.35	0.44	0.58	0.70
2	0.25	0.26	0.36	0.41	0.44	0.49
3	0.03	0.06	0.22	0.38	0.45	0.80
4	0.33	0.35	0.48	0.45	0.49	0.43
5	0.11	0.30	0.40	0.41	0.45	0.55
Chloramphenical	-0.10	-0.17	-0.18	-0.19	-0.19	-0.18
Gentamycin	-0.10	-0.14	-0.16	-0.16	-0.15	-0.9

Table 9: Comparison of ABTS, DPPH and superoxide radicals assays for estimating antioxidant activity of piperidine-4-ones **1-5**

Compds	ABTS radical (IC_{50} /mL)	DPPH radical (IC_{50} /mL)	Superoxide radical (IC_{50}/mL)
1	45.72	39.15	75.29
2	90.21	32.78	34.24
3	63.49	32.95	30.50
4	18.64	24.42	35.374
5	56.38	37.13	11.200
Rutin	**5.13**	**5.79**	**4.49**
BHT	**6.14**	**6.30**	**5.59**

Table: 10. Glide Extra-precision (XP) Results

Compounds	Glide Score	Glide Energy	No. of H bond interactions	Interacting Residue	Distance (Å)	Hydrogen bond donor	Hydrogen bond Acceptor
1	-5.710	-47.773	1	ASN 59	2.11	A: ASN 59: (H)H	Ligand: (O)
2	-2.473	-31.039	2	GLU 17	2.18	A: GLU 17: (H)H	Ligand: (O)
				LYS 38	2.35	A: LYS 38 : (H)HZ3	Ligand: (O)
3	-4.416	-53.504	1	CYS 87	-	A: CYS 87: (H)H	Ligand: (O)
4	-2.840	-21.835	-	-	-	-	-
5	-3.892	-16.751	1	LYS 38	2.46	A: LYS 38 : (H)HZ3	Ligand: (O)

Table captions